Enhanced Stability of Core−Surface Cross-Linked Micelles Fabricated from Amphiphilic Brush Copolymers

Peisheng Xu,[†] Huadong Tang,[†] Shiyan Li,[‡] Jun Ren,[‡] Edward Van Kirk,[§] William J. Murdoch,[§] Maciej Radosz,[†] and Youqing Shen*,[†]

Department of Chemical & Petroleum Engineering, School of Pharmacy, and Department of Animal Science, University of Wyoming, Laramie, Wyoming 82071

Received February 29, 2004; Revised Manuscript Received May 18, 2004

"Stealth" nanoparticles made from polymer micelles have been widely explored as drug carriers for targeted drug delivery. High stability (i.e., low critical micelle concentration (CMC)) is required for their intravenous applications. Herein, we present a "core−surface cross-linking" concept to greatly enhance nanoparticle's stability: amphiphilic brush copolymers form core−surface cross-linked micelles (nanoparticles) (SCNs). The amphiphilic brush copolymers consisted of hydrophobic poly(ϵ-caprolactone) (PCL) and hydrophilic poly(ethylene glycol) (PEG) or poly(2-(*N*,*N*-dimethylamino)ethyl methacrylate) (PDMA) chains were synthesized by macromonomer copolymerization method and used to demonstrate this concept. The resulting SCNs were about 100 times more stable than micelles from corresponding amphiphilic block copolymers. The size and surface properties of the SCNs could be easily tailored by the copolymer's compositions.

Introduction

Over the past decades, targeted drug delivery has been widely explored to deliver drugs specifically to tissues, especially cancerous tissues, for enhanced therapeutic efficacy and reduced systemic toxicity. For example, polymer−drug conjugates,[1−3] dendrimers,[4−6] liposomes,[7−9] polymer micelles,[10−15] and polymer nanoparticles[16−19] have been demonstrated to preferentially carry drugs to cancerous tissues, resulting in much improved therapeutic efficacies. Cancer targeting was achieved by the enhanced permeability and retention (EPR) effect: tumor's permeable capillaries and poor lymphatic drainage cause trapping of macromolecules and colloidal particles in cancerous tissues.[20−26] Hence, the resulting drug concentrations in tumors could be as much as 1 order of magnitude higher than that in healthy tissues.[26,27]

Of the various drug carriers, polymer nanoparticles have been attracting much attention because of their ability to preferentially deliver drugs to cancer cells.[11,17−19] Nanoparticles are submicron colloidal particles. Due to their subcellular size, nanoparticles can penetrate through fenestrations of capillaries, accumulate within the interstitial space, and be taken up by cells via endocytosis.[23] Nanoparticles with a hydrophilic surface (e.g., polymer micelles with poly(ethylene glycol) outer layers) can evade recognition by the reticuloendothelial system (RES), and thus have a prolonged circulatory time and accumulation in tumors.[15,28,29] They are generally more stable with circulation than liposomes. Drugs entrapped within their cores are protected from peripheral metabolism. Nanoparticles have thus been used as carriers of drugs, e.g., cisplatin,[30] doxorubicin (DOX),[31] adriamycin,[32,33] and paclitaxel,[34−36] to treat cancers for enhanced therapeutic efficacy and reduced toxicity to the body. For example, encapsulated doxorubicin in PEG−poly(aspartic acid) micelles at doses of 50 mg/kg inhibited tumor growth in a drug resistant murine colon carcinoma model, whereas a 20 mg/kg dose of doxorubicin resulted in toxic deaths.[37]

One special type of nanoparticle is polymer micelles formed from amphiphilic copolymers. Amphiphilic copolymers composed of hydrophilic and hydrophobic segments form a micellar structure in water with a hydrophobic compact inner core and a hydrophilic outer corona. The size depends on the lengths of the hydrophilic and hydrophobic chains but generally is in the submicron range.[10,17] The hydrophilic outer layer acts as a shelter to protect the inner hydrophobic core from being recognized and cleaned by RES and other clearing organs such as the kidneys, liver, spleen, and lung.[17] The hydrophilic corona is stable on the core surface due to the covalent linking. Thus, these type nanoparticles, also named "stealth nanoparticles", have a long circulation time necessary for passive targeting to cancerous tissues via the EPR effect.[17]

For intravenous application, it is critical that the micelles are stable, i.e., have low critical micelle concentration (CMC). Otherwise, the micelles will disassociate into unimers upon dilution in the bloodstream, causing nontargeted drug release and toxicity. The way used to increase the stability of micelles is to chemically cross-link their cores after the core formation (Figure 1a).[38] Such micelles do not disassociate, but chemical reactions in the cores are undesirable because they may alter the structures and properties of the encapsulated drugs.

Herein, we report highly stable core-surface cross-linked micelles (nanoparticles) (SCNs) made from amphiphilic polymer brushes. The backbones of the polymer brushes act

* To whom correspondence should be addressed.
[†] Department of Chemical & Petroleum Engineering.
[‡] School of Pharmacy.
[§] Department of Animal Science.

10.1021/bm049874u CCC: $27.50
Published on Web 07/21/2004

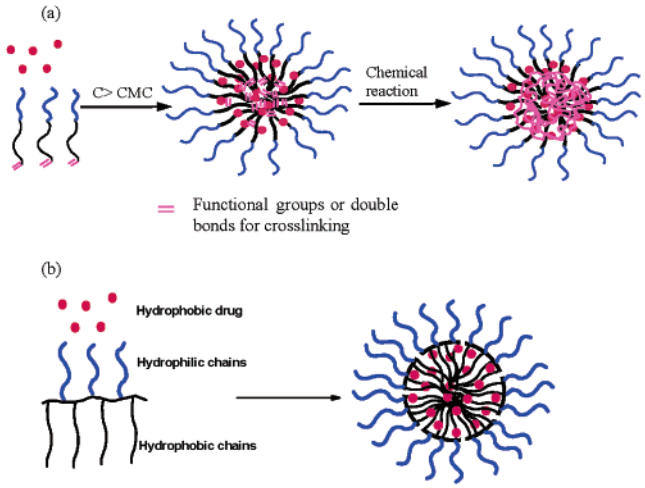

Figure 1. Formation of core-cross-linked micelles by chemical reactions (a) and core−surface cross-linked micelles (SCNs) from amphiphilic brush polymers (b).

Scheme 1. Synthesis of PCL Macromonomer (mPCL)

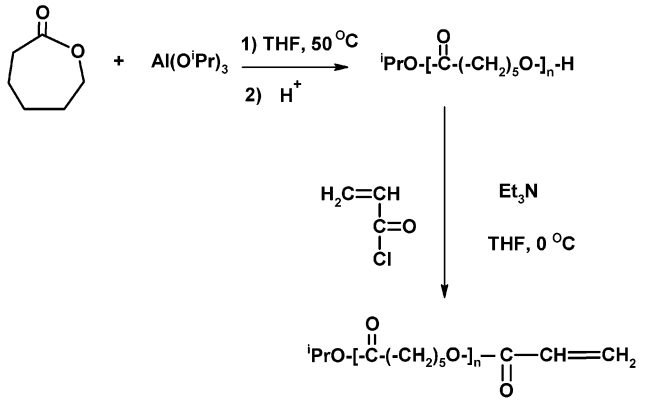

as cross-links on the hydrophobic core surface to greatly enhance the stability of the micelles (Figure 1b) without using chemical reaction in the core. Brush copolymers with polycaprolactone (PCL) as hydrophobic chains and poly(ethylene glycol) (PEG) or poly(2-(*N*,*N*-dimethylamino)ethyl methacrylate) (PDMA) as hydrophilic chains were synthesized by the macromonomer copolymerization method and used to fabricate SCNs. PCL is a nontoxic biodegradable polymer, which can be biodegraded in the Krebs cycle into soluble nontoxic oligomers.[39] PEG is a nonimmunogenic nontoxic water-soluble polymer, which is hydrophilic and known to prevent interactions with proteins.[40] PDMA is partially positively charged in water. Micelles with PDMA chains have a positively charged hydrophilic surface, which may facilitate the cellular uptake by adsorption mediated endocytosis. [41]

Experimental Section

Materials. ϵ-Caprolactone (ϵ-CL) (Aldrich) was dried over calcium hydride with stirring for 24 h at room temperature. PCL macromonomer (m-PCL: $M_n = 3.8 \times 10^3$; $M_w/M_n = 1.07$) was synthesized (Scheme 1) according to litersture.[42] Poly(ethylene glycol) methyl ether methacrylate 50% solution in water (Aldrich) (mPEG, $M_n = 2080$) was dried under a high vacuum with a rotary evaporator. Tetrahydrofuran

Scheme 2. Synthesis of ATRP Initiator HBMPA

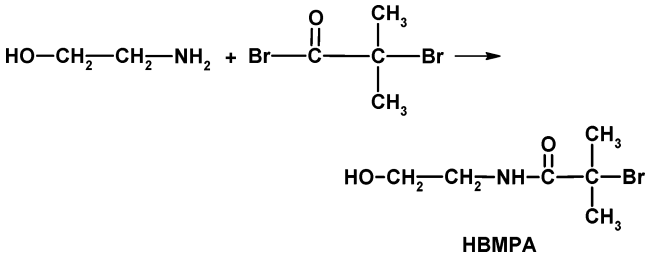

(THF) was dried by refluxing over calcium hydride. CuBr was stirred in glacial acetic acid, filtered, and washed with absolute ethanol as well as diethyl ether. 1,1,4,7,10,10-Hexamethyltriethylenetetramine (HMTETA, 97%), methyl α-bromophenylacetate (MBP, 97%), acryloyl chloride (96%), triethylamine (Et_3N, 99.5%), *N*,*N*-dimethylformamide (DMF, 99.8%), *N*-phenyl-1-naphthylamine (PNA), and 2-(*N*,*N*-dimethylamino)ethyl methacrylate (DMA), all from Aldrich, were used as received without further purification.

Instrumentation. Gel permeation chromatography (GPC) was used to determine polymer molecular weights and molecular weight distribution (PDI) using polystyrene standards (Polysciences Corporation). The measurements were operated on a Waters SEC equipped with a Waters 2414 refractive index detector and two 300 mm Solvent-Saving GPC Columns (molecular weight ranges: $5 \times 10^2-3 \times 10^4$, $5 \times 10^3-6 \times 10^5$, at a flow rate of 0.30 mL/min) using THF as solvent at 30 °C. Data were recorded and processed using a Waters software package. ^{1}H NMR spectra were recorded on a Bruker Avance DRX-400 spectrometer using $CDCl_3$ as solvent. Chemical shifts were reported downfield from 0.00 ppm using TMS as internal reference. Micelle sizes were determined by dynamic laser light scattering (DLS, Nicomp 370 particle sizer). The measurement of the PNA excitation was carried out with the fluorescence spectroscopy (SPECTRAmax GEMINI XS spectrofluorometer, Molecular Devices). Excitation wavelength was 340 nm for the measurement of emission spectra. Sensitivity was set at 10. The emission intensity at 418 nm was recorded with the cutoff wavelength at 420 nm to estimate CMC.

Synthesis of ω-Methacryloyl Poly(2-(*N*,*N*-dimethylamino)ethyl methacrylate) Macromonomer (mPDMA). mPDMA was prepared by a two step reaction: the synthesis of ω-hydroxy-PDMA by atom transfer radical polymerization (ATRP)[43] of DMA and subsequent reaction with methacrylic acid (Schemes 2 and 3).

Synthesis of the N-(2-Hydroxyethyl)-2-bromo-2-methylpropionamide (HBMPA) as the Initiator for the ATRP of DMA (Scheme 2). Ethanolamine (9.1 mL, 0.15 mol) and THF (150 mL) were charged to a three neck flask. The mixture was cooled to 0 °C. 2-Bromoisobutyryl bromide (9.3 mL, 0.075 mol) was added dropwise with stirring. The reaction mixture was kept at 0 °C for 4 h, and then stirred at room-temperature overnight. After THF was removed by rotary evaporation, the residue was dissolved in dichloromethane and washed with deionized water. The organic layer was collected and dried over $CaCl_2$. The removal of dichloromethane and distillation under vacuum yielded HBMPA. ^{1}H NMR (400

Scheme 3. Synthesis of PDMA Macromonomer (mPDMA)

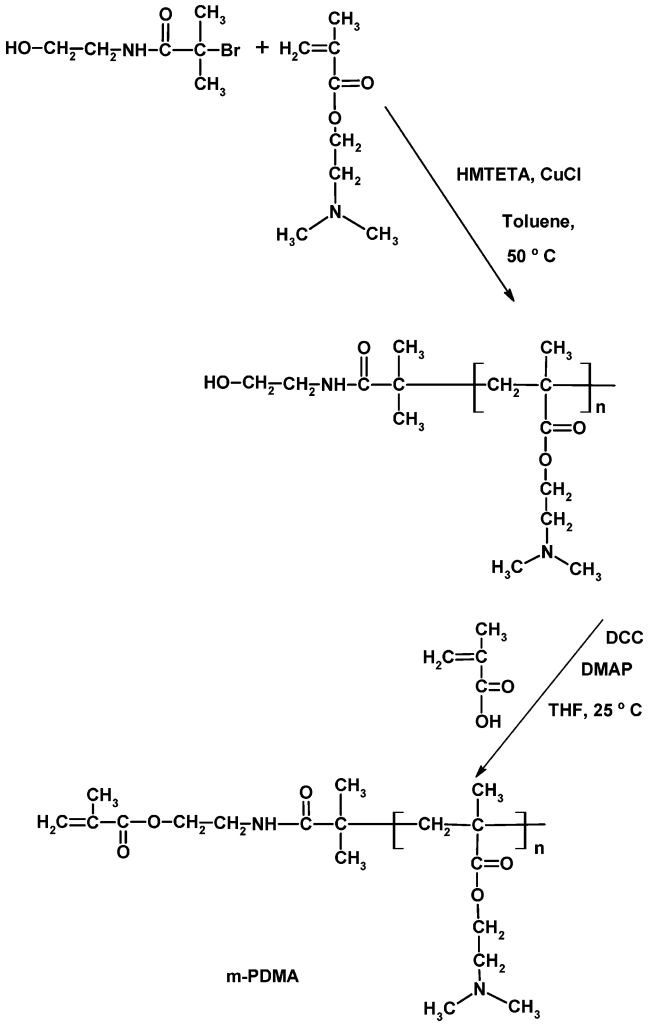

MHz, $CDCl_3$): δ 7.14 (s, 1H), 3.76 (t, 2H), 3.46 (t, 2H), 1.98 (s, 6H), 1.85 (s, 1H).

Synthesis of ω-Hydroxy-PDMA by ATRP. The ATRP used CuCl/HMTETA as the catalyst and HBMPA as the initiator at [monomer]/[initiator] ratio of 20/1 (molar) and HMTETA/CuCl/HBMPA of 1/1/1(molar).[43] A typical preparation is as follows: DMA (5.4 mL, 26.6 mmol), HMTETA (0.35 mL, 1.33 mmol), CuCl (0.126 g, 1.33 mmol), and degassed toluene (2.5 mL) were charged into a Schlenk tube. The mixture was degassed by nitrogen purging for 10 min. The initiator HBMPA (0.267 g, 1.33 mmol) was dissolved in 2.9 mL of toluene and degassed for 5 min. This initiator solution was added by a syringe to the Schlenk tube, and the tube was immersed in 50 °C water bath for 28 min. Then the reaction was terminated by adding $CuCl_2$ and hexane was added to precipitate out PDMA polymer. The polymer was redissolved in toluene, and the solution was passed through columns of silica gel twice to remove the residual copper catalyst. The PDMA macromonomer precursor was dried under vacuum for 24 h ($M_n = 7.4 \times 10^3$, $M_w/M_n = 1.09$).

Synthesis of mPDMA Macromonomer (Scheme 3). The macromonomer was prepared by the reaction of methacrylic acid with ω-hydroxy PDMA. A typical synthesis is as follows: ω-hydroxy PDMA ($M_n = 7.4 \times 10^3$, 3.489 g, 0.47 mmol), methacrylic acid (80 μL, 0.94 mmol), dicyclohexylcarbodiimide (0.193 g, 0.94 mmol), 4-(dimethylamino)-pyridine (5.8 mg, 0.047 mmol), and THF (40 mL) were stirred at room temperature for 24 h. After the precipitate was removed by filtration, the filtrate was concentrated by rotary evaporation. The polymer was precipitated into 10-fold of hexane and purified by reprecipitation. The macromonomer was dried under vacuum for 24 h.^{1}H NMR (400 MHz, $CDCl_3$): δ (ppm): 6.08 (s, weak)), 5.53 (s, weak), 2.63 (t), 2.29 (s), 1.96 (m), 1.00 (d).

Synthesis of brush copolymers by macromonomer copolymerization (Schemes 4 and 5). *Free Radical Copolymerization of mPCL and mPEG.* mPCL ($M_n = 3.8 \times 10^3$, 0.493 g, 0.13 mmol), mPEG ($M_n = 2.08 \times 10^3$, 0.270 g, 0.13 mmol), and AIBN (2.1 mg, 0.013 mmol) were charged in a Schlenk tube. The mixture was degassed by vacuum/nitrogen purging for three cycles. Degassed DMF (2 mL) was added by syringe. The mixture was heated in a 40 °C water bath for 2 min, and a clear solution was formed. The solution was degassed again for 5 min with stirring, and then the tube was immersed in a 60 °C water bath. At different time intervals, polymer samples were taken using degassed syringes and diluted in 0.1 mL of $CDCl_3$. The polymer molecular weight, the polydispersity, and the conversion of the reaction were measured by GPC. The reaction mixture was dissolved in DMF and then precipitated in a 10-fold methanol/ethyl ether (1:1, v/v) mixture to remove the unreacted macromonomer. The final product was isolated and dried under vacuum for 48 h. The PCL/PEG chain ratio was measured with ^{1}H NMR by the intensity ratio of the CH_2 signal in PEG (3.62 ppm) and PCL (4.03 ppm).[44]

Scheme 4. Synthesis of PCL/PEG Brush Copolymer by (a) Free Radical Polymerization and (b) Atom Transfer Radical Polymerization (ATRP)

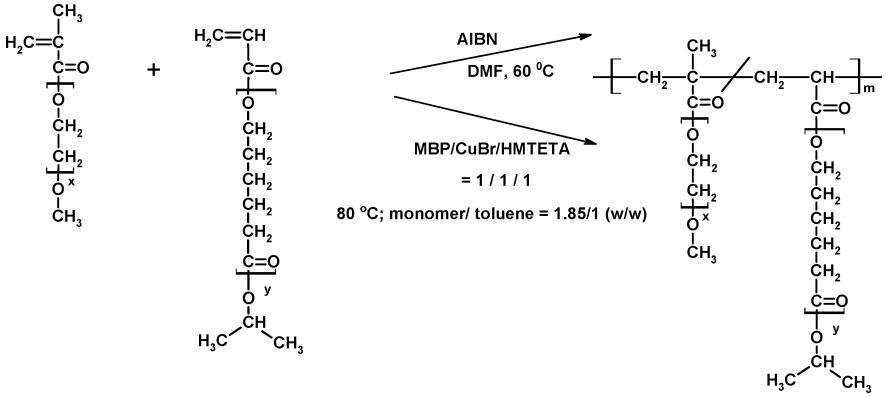

Scheme 5. Synthesis of PCL/PDMA Brush Copolymer by Free Radical Polymerization.

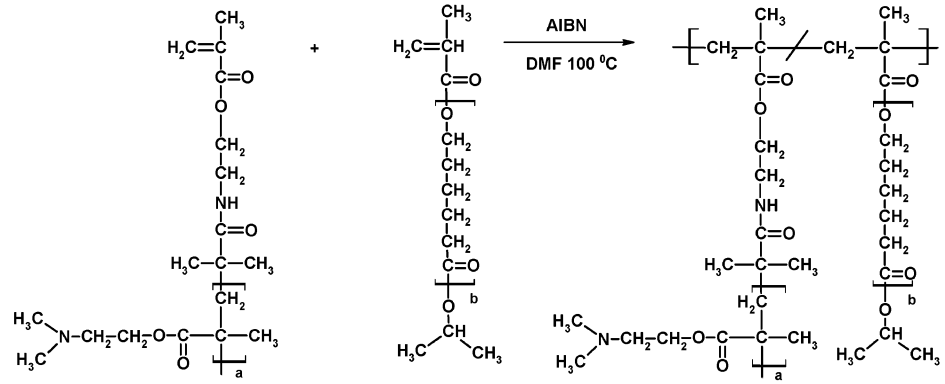

The conversions of the macromonomers were calculated by areas in the GPC trace of the reaction mixture according to the calibration curve. The calibration curve was developed by a least-squares method assuming that the area under the GPC trace curve is proportional to the weight of each component. A series of mixtures of the copolymer, mPCL, and mPEG with known composition ratio were measured with GPC. The area of each peak in the GPC traces of the mixtures was calculated by GPC software, and the least-squares method was then used to develop a model having the minimal deviation from their real compositions. The conversion of each macromonomer in the copolymerization was calculated from the relative peak area ratio in the GPC traces according to the calibration curve.

Free Radical Copolymerization of mPCL and mPDMA. mPCL ($M_n = 7.0 \times 10^3$, 0.13 g, 0. 0186 mmol), mPDMA ($M_n = 8.0 \times 10^3$, 0.20 g, 0.025 mmol), and AIBN (3.3 mg, 0.02 mmol) were charged to a Schlenk tube. The mixture was degassed by vacuum/nitrogen purging for three cycles. Degassed DMF (0.5 mL) was added by a syringe. The mixture was heated in a 40 °C water bath for 2 min until a clear solution was formed. This solution was degassed again for 5 min with stirring, and then the tube was put into a 100 °C oil bath. At different time intervals, polymer samples were taken using degassed syringes and diluted in 0.1 mL of $CDCl_3$ solution. The molecular weight and polydispersity of the polymer were measured by GPC. The reaction mixture was dissolved in DMF and then precipitated in a 10-fold methanol/ethyl mix solvent (1/1 v/v) to remove the unreacted macromonomer. The final product was isolated and dried under vacuum for 48 h.

Synthesis of Brush Copolymers by Atom Transfer Radical Copolymerization (ATRP). The ATRP copolymerization of mPEG and mPCL used CuBr/HMTETA as the catalyst and methyl α-bromophenylacetate (MBP) as the initiator at [monomer]/[initiator] (molar) of 5/1 and HMTETA/CuBr/MBP of 1/1/1. A typical preparation is as follows: mPCL ($M_n = 5.7 \times 10^3$, 0.371 g, 0.065 mmol), mPEG ($M_n = 2.08 \times 10^3$, 0.405 g, 0.195 mmol), HMTETA (14 μL, 0.052 mmol), and CuBr (7.6 mg, 0.052 mmol) were charged to a Schlenk tube. The mixture was degassed by vacuum/nitrogen purging for three cycles. Degassed toluene (0.5 mL) was added by a syringe. The mixture was heated in a 40 °C water bath for 2 min, and a clear solution was formed. This solution was degassed again for 5 min under stirring. The initiator MBP (8.2 μL, 0.052 mmol) was added by a syringe, and then the tube was immersed in an 80 °C water bath. At different time intervals, polymer samples were taken using degassed syringes and diluted in 0.1 mL of $CDCl_3$ containing $CuBr_2$. The reaction mixture was dissolved in toluene and passed through a silica gel column to remove the copper catalyst. The product was further purified as described in the free radical process. The conversion was measured by GPC as described above.

PCL-PEG Block Copolymer Synthesis. PCL-PEG block copolymer was synthesized by PEG macroinitiator method. A typical polymerization is as follows: PEG ($M_n = 2.0 \times 10^3$, 8.0 g, 4.0 mmol) was added to 500 mL of dried toluene. Aluminum isopropoxide−toluene solution (0.0569 g Al(^{i}-OPr)$_3$/mL toluene solution. 13.0 mL, 3.6 mmol) was added to the flask. The mixture was refluxed for 5.5 h and concentrated to 10 mL by distillation to produce the PEG macroinitiator. This macroinitiator was dissolved in dried toluene for use in the next step.

The ring-opening polymerization was carried out as follows: dried ϵ-CL (1.3 mL, 12.1 mmol) was added to a predried Schlenk tube; 1.0 mL of PEG macroinitiator toluene solution (0.40 g, 0.20 mmol) was added via a degassed syringe at [ϵ-CL]/[catalyst] of 60/1(molar) and [ϵ-CL]/[toluene] of 1/1 (v/v). The mixture was put into a 35 °C water bath for 9 min. The product was further purified as described above in the free radical copolymerization process. The CL/EG ratio was measured with ^{1}H NMR by the ratio of the CH_2 signal intensity in PEG (3.62 ppm) and PCL (4.03 ppm) and the molecular weight was then calculated (PEG-(2.0×10^3)-*block*-PCL(6.2×10^3)). The polydispersity was 1.21.

Micelle Preparation and Characterization. The micelles were prepared using a solvent displacement method with an acetone−water system. In a typical procedure, the copolymer (10 mg) was dissolved in 2.5 mL of acetone with stirring for about 2 h. The polymer acetone solution was added dropwise into 20 mL of deionized water with stirring, and the mixture was continually stirred overnight to form micelles. The suspension was stirred under reduced pressure for 8 h to remove acetone. The solution was filtrated through 0.2 μm syringe filters before any measurement.

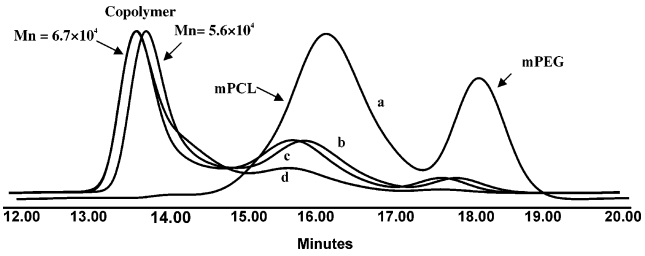

Figure 2. GPC traces of the copolymerization mixture of mPCL (M_n, 3.8×10^3) and mPEG (M_n, 2.08×10^3) via free radical polymerization. Reaction conditions: 60 °C; [monomer]/[AIBN]=20/1; [mPCL]/[mPEG] = 1/1(molar); [monomer]/[DMF] = 0.40/1(w/w). Reaction time: 1 h (a), 6.5 h (b), 19.2 h (c), 106 h (d).

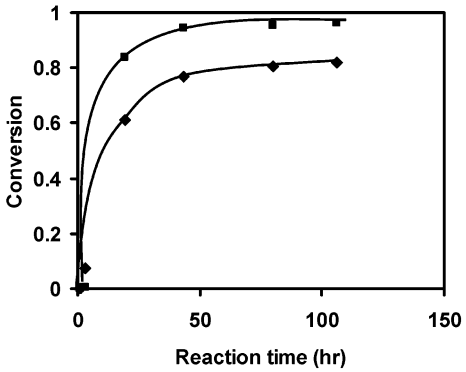

Figure 3. Copolymerization kinetics of mPCL (M_n, 3.8×10^3) and mPEG (M_n, 2.08×10^3) via free radical polymerization. PEG (■); PCL-(◆). See Figure 2 for reaction conditions.

Micelle Size Measurement. The particle size was measured by dynamic light scattering (DLS), which was performed on a Nicomp 370 particle sizer with a wavelength of 514.5 nm at a fixed scattering angle of 90°. Data were analyzed by Nicomp software (version 12.3) with volume-weighted Gaussian/Nicomp analysis mode, which gave histograms of relative volume vs mean diameter.

Critical Micelle Concentration (CMCs) Measurements. CMCs of the copolymers were estimated by a fluorescence spectroscopic method using *N*-phenyl-1-naphthylamine (PNA) as the fluorescence probe. Typically, PNA solutions in acetone were added to each brown bottle. Acetone was then evaporated, leaving 1.0×10^{-8} mol of PNA in each bottle. Aqueous solutions (10 mL) of PCL/PEG or PCL/PDMA brush copolymer at concentrations ranging from 0.25 g/L to 0.05 mg/L were added to the bottles. The mixtures were stirred at 60 °C for 3 h. They were sonicated for 1 min before measurement. The spectroscopy measurement was carried out at the emission wavelength of 418 nm and excitation wavelength of 340 nm.[45]

Results and Discussion

Preparation of PCL/PEG Brush Copolymers. The copolymerization of the mPCL and mPEG was first carried out via free radical polymerization in DMF using AIBN as initiator (Scheme 4). Because the molecular weights of the macromonomers were high ($M_{n,mPCL} = 3.8 \times 10^3$, $M_{n,mPEG} = 2.08 \times 10^3$), the double bond concentration was very low, total 0.13 mol/L. We used a high initiator concentration ([monomer]/[initiator] = 20/1 (molar ratio)) to increase the polymerization rate. The GPC traces of the polymerization mixture are shown in Figure 2. The intensities of mPEG and mPCL peaks decreased, and a new copolymer peak appeared at a higher molecular weight region. The conversions of the macromonomers were calculated by the calibration curve using the relative areas of the peaks in the GPC traces. Figure 3 shows the conversions of mPCL and mPEG as a function of time. mPCL had lower reactivity than mPEG. For example, the conversions of mPCL and mPEG were about 82% and 96%, respectively, after 106 h of polymerization. The lower reactivity of mPCL may be ascribed to its higher molecular weight. The composition of the copolymer was measured with NMR by the ratio of the CH_2 signal intensity in polymer (3.62 and 4.03 ppm).[44] A typical spectrum is shown in Figure 4. The signals of the backbones are overlapped by those of the side chains.

Figure 2 shows that the mPCL and mPEG copolymers produced by free radical copolymerization had almost

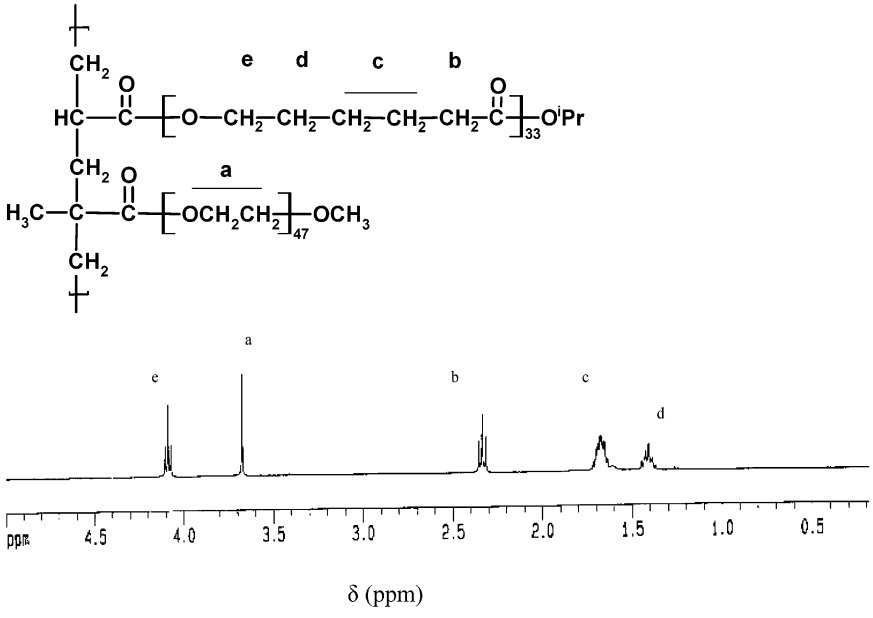

Figure 4. ^{1}H NMR spectrum of PCL/PEG brush copolymers

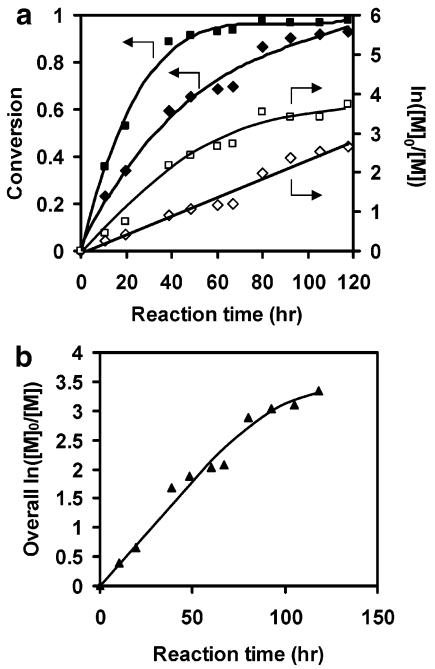

Figure 5. Copolymerization of mPCL (M_n, 5.7 × 10^3) and mPEG (M_n, 2.08 × 10^3) catalyzed by CuBr/HMTETA at 80 °C in toluene. $[PCL]_0/[PEG]_0/[MBP]_0/[CuBr]_0/[HMTETA]_0$ =25/75/20/20/20(in moles). [monomer]/[toluene] = 1.85/1 (w/w). mPEG (■,□); mPCL(◆,◇); overall (mPCL + mPEG) (▲).

constant molecular weight at different conversions, indicative of no control in backbone chain lengths, which is typical of free radical polymerization. We thus also used atom transfer radical polymerization (ATRP), a versatile living radical polymerization,[46] for the copolymerization of the macromonomers to control the backbone length (Scheme 4b). Figure 5 shows the kinetics of the ATRP copolymerization of mPCL and mPEG. The $\ln([M]_0/[M]) \sim t$ plots for mPEG, mPCL, and overall (mPEG + mPCL) were linear at low conversions. Similar to the free radical copolymerization, the polymerization of mPCL was slightly slower than that of mPEG. For example, the conversion of the mPCL was about 92% and that of mPEG was 97% after 118 h polymerization. Compared with free radical polymerization, ATRP could reach higher conversions for both mPCL and mPEG, probably because of less radical termination. This made it easy to tailor the copolymer composition simply by adjusting the PCL/PEG feeding ratio.

Different from the free radical copolymerization, the GPC traces show that the resulting copolymer gradually shifted to the high molecular weight region, and thus the calculated molecular weight increased as the conversion increased (Figures 6 and 7). Since the molecular weights of the copolymers were calculated based on PS standards using a refractive index detector, they were lower than their true values because branched polymers have smaller hydrodynamic volumes than corresponding linear counterparts with the same molecular weights. The M_n of the copolymers leveled off at high conversion. The polydispersity of resulting copolymers via ATRP was low, about 1.35.

High concentrations of catalyst and initiator were found to be necessary for high yields in this macromonomer copolymerization. For example, at [monomer]/[CuBr]/[initiator] = 50/1/1, GPC did not detect any copolymer after 36 h of polymerization. This is caused by the low concentration and low activities of the terminal double bonds of the macromonomers due to their long chains.

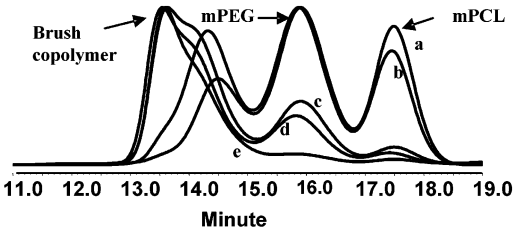

Figure 6. GPC traces of the copolymerization mixture of mPCL and mPEG via ATRP polymerization. See Figure 5 for reaction conditions. Reaction time: 10.7 h (a); 19.3 h (b); 48.5 h (c); 80 h (d); 118 h (e).

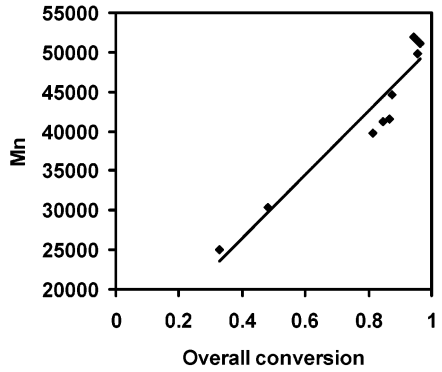

Figure 7. Molecular weight of the brush copolymer as a function of overall conversion of mPCL and mPEGr via ATRP catalyzed by CuBr/HMTETA at 80 °C in toluene. See Figure 5 for reaction conditions.

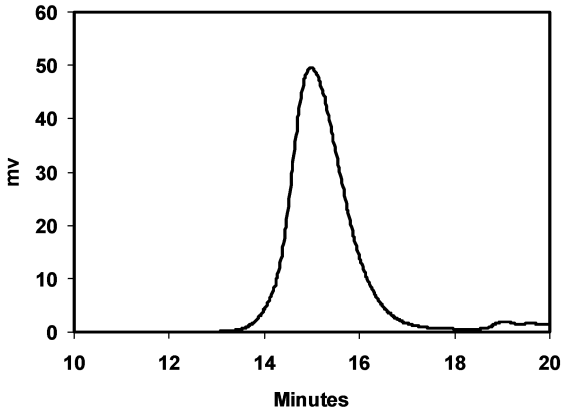

Figure 8. GPC trace of the copolymerization mixture of mPCL (M_n, 7.0 × 10^3) and mPDMA (M_n, 8.0 × 10^3) via free radical polymerization at reaction time of 174.5 h. Reaction conditions: 80 °C; [mPDMA]/[mPCL] = 1:3, [monomer]/[initiator] =5/2, [monomer]/[DMF] = 0.77/1(w/w); copolymer M_n, 1.8 × 10^4.

Preparation of PCL/PDMA Brush Copolymers. The mPDMA macromonomer was synthesized by a three-step method (Schemes 2 and 3). First, HBMPA was synthesized by the reaction of 2-bromoisobutyryl bromide with ethanolamine. It initiated the polymerization of DMA to produce PDMA with a terminal hydroxy group. Methacrylic acid reacted with ω-hydroxy PDMA to produce mPDMA.

The copolymerization of mPCL and mPDMA was carried out via free radical polymerization in DMF using AIBN as the initiator (Scheme 5). A typical GPC trace of the PEG/PDMA brush copolymer is shown in Figure 8. Similar to the PCL/PEG copolymerization, the polymerization required

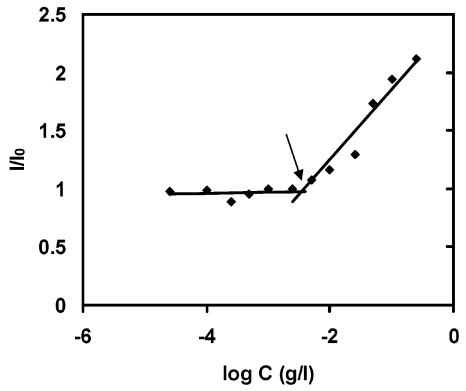

Figure 9. Intensity ratio I/I_0 in PNA fluorescence emission spectra as a function of logc of the PCL/PEG (1/3) brush copolymer in distilled water. [PNA] = 1.0×10^{-6} M (I/I_0 is the relative fluorescence intensity in the presence of PNA (I) and the absence (I_0) of PNA).

Table 1. Critical Micelles Concentrations (CMCs) of the Brush Copolymers of PCL (M_n, 7.0×10^3) with PEG (M_n, 2.08×10^3) or PDMA (M_n, 8.0×10^3)

copolymers	PCL/PEG or PCL/PDMA chain ratio	M_n ($\times 10^3$)	CMC (g/L) ($\times 10^{-3}$)	CMC (mol/L) ($\times 10^{-8}$)
PCL-PEG block	1:1.0	8.2	40	480
PCL/PEG brush	1:0.93	21	1.0	5.0
PCL/PEG brush	1:3.0	48	3.8	7.9
PCL/PDMA brush	1:0.42	–	6.3	35

a high initiator concentration and was very slow, but both of the macromonomers could be completely consumed, as shown in Figure 8. Thus, the resulting brush copolymers did not require purification, and the copolymer composition was essentially the same as the feeding ratio.

Micelle Formation. The formation of micelles of the brush copolymers was detected using *N*-phenyl-1-naphthylamine (PNA) as a fluorescent probe. PNA has a high fluorescence activity in nonpolar environments, but polar solvents such as water can quench its fluorescence.[47] We found that PNA was a much better fluorescent probe than pyrene in terms of reproducibility (Figure 9). The measured CMCs of the micelles of the brush copolymers are shown in Table 1. The CMC of the block copolymer with the same chain lengths of PCL and PEG as those in the brush copolymers was also measured for comparison. The PCL/PEG ratio only slightly affected the CMCs. With more PEG chains, the CMC of the brush copolymer only increased slightly (Table 1). For instance, the CMC of the copolymer with a PCL/PEG ratio of 1/3 was 3.8 mg/L, compared with 1.0 mg/L of the copolymer with the ratio of 1/0.93. This makes it possible to tailor the hydrophilic chain density on the nanoparticle surface, which strongly affects its pharmacokinetics and biodistribution,[17] without changing its stability.

Most significantly, the brush copolymers have much lower CMCs than corresponding block copolymers. For example, the CMC of the brush copolymer with PCL/PEG chain ratio of 1/0.93 was almost 40 times (100 times if using molar concentration) lower than that of the block copolymer (chain ratio of 1/1). Even the brush copolymer with more PEG (e.g., PCL/PEG = 1/3) had a much lower CMC than that of the block copolymer, indicative of the much improved stability

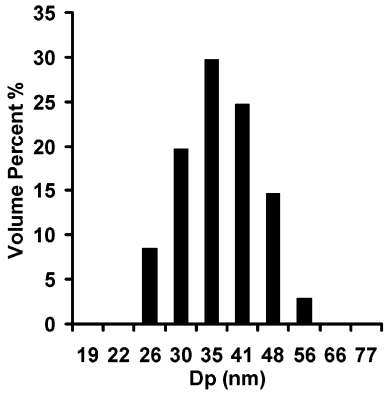

Figure 10. Size distribution of the micelles of a PCL/PEG (1/1.09) brush copolymer. M_n, 9.2×10^3; mPCL (M_n, 3.8×10^3), mPEG (M_n, 2.08×10^3)).

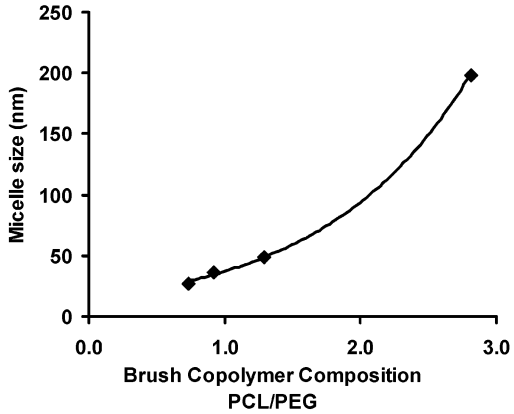

Figure 11. Dependence of the micelles size on the PCL/PEG chain ratio of the brush copolymers made of mPCL (M_n, 3.8×10^3) and mPEG (M_n, 2.08×10^3).

of the micelles formed from the brush copolymers. We believe that the improved stability of the micelles of the brush copolymers is derived from the partially cross-linking on the core surface, as shown in Figure 1b. Table 1 shows that the M_n of the brush copolymers was about 3−6 times of that of the block copolymer. This was equivalent to three to six block copolymer chains linked together by the copolymer backbone on the micelle surface, entailing much improved stability of the micelles. Thus, the micelles less likely disassociate in the bloodstream. Meanwhile, there is no chemical reaction involved in the core. The properties of drugs encapsulated in the cores will not be altered.

Micelle Size. A solvent-displacement method was used to fabricate the micelles from the synthesized polymer brushes. Figure 10 shows that the micelles had a very narrow size distribution. The diameter of micelles depends on the hydrophobic/hydrophilic chain ratio: it increased with increasing PCL/PEG chain ratio (Figure 11). For example, the micelles formed from the copolymer with PCL/PEG ratio of 2.81 had a diameter of 198 nm, whereas the diameter of the micelles was 27.4 nm at the PCL/PEG ratio of 0.73. Similarly, the micelles had a 54.7 nm diameter at a PCL/PDMA ratio of 2.38. Thus, the size of micelles of the brush copolymers can be easily tailored by changing the hydrophobic/hydrophilic chain ratio without sacrificing micelle stability because it only slightly alters the CMCs.

In addition, PDMA is partially positively charged in water. The micelles formed by the PCL/PDMA brush copolymer thereby had a positively charged hydrophilic corona, which may be used to facilitate the cellular uptake of the nanoparticles by electrostatic interaction with the negatively charged cell membrane.[41] The surface property of the nanoparticles thus can be changed simply by using different hydrophilic chains.

Conclusions

The results have demonstrated that core−surface cross-linked micelles fabricated from amphiphilic brush copolymers had much improved stability with easily adjustable sizes and surface properties by the hydrophobic/hydrophilic chain ratio and the type of the hydrophilic chains. This method provides a new approach to designing "stealth" stable nanoparticles without chemical reactions in the cores for targeted drug delivery. The synthesis of totally degradable brush copolymers for degradable core−surface cross-linked nanoparticles and their applications in drug delivery are under way.

Acknowledgment. We thank the University of Wyoming EPSCoR and National Science Foundation (BES-0401982) for the financial support.

References and Notes

(1) (a) Putnam, D.; Kopeček, J. Polymer conjugates with anticancer activity. *Adv. Polym. Sci*. **1995**, *122*, 55−123. (b) Kopeček, J.; Kopeckova, P.; Minko, T.; Lu, Z. R.; Peterson, C. M. Water soluble polymers in tumor targeted delivery. *J. Controlled Release* **2001**, *74*, 147−158.

(2) Peterson, C. M.; Lu, J. M.; Sun, Y.; Peterson, C. A.; Shiah, J.-G.; Straight, R. C.; Kopeček, J. Combination chemotherapy and photodynamic therapy with *N*-(2-hydroxypropyl)meth acrylamide copolymer-bound anticancer drugs inhibit human ovarian carcinoma heterotransplanted in nude mice. *Cancer Res*. **1996**, *56*, 3980−3985.

(3) Murthy, N.; Campbell, J.; Fausto, N.; Hoffman, A. S.; Stayton, P. S. Design and synthesis of pH-responsive polymeric carriers that target uptake and enhance the intracellular delivery of oligonucleotides. *J. Controlled Release* **2003**, *89*, 365−374.

(4) Liu, M.; Kono, K.; Frechet, J. M. J. Water-soluble dendritic unimolecular micelles: Their potential as drug delivery agents. *J. Controlled Release* **2000**, *65*, 121−131.

(5) Baker, J. R.; Quintana, A.; Piehler, L.; Banazak-Holl, M.; Tomalia, D.; Raczka, E. The synthesis and testing of anticancer therapeutic nanodevices. *Biomed. Microdevices* **2001**, *3*, 61−69.

(6) Ihre, H. R.; Padilla, D. J.; Omayra, L.; Szoka, F. C., Jr.; Frechet, J. M. J. Polyester dendritic systems for drug delivery applications: Design, synthesis, and characterization. *Bioconjug. Chem.* **2002**, *13*, 443−452.

(7) Drummond, D. C.; Meyer, O.; Hong, K.; Kirpotin, D. B.; Papahadjopoulos, D. Optimizing liposomes for delivery of chemotherapeutic agents to solid tumors. *Pharmacol. Rew*. **1999**, *51*, 691−743.

(8) Booser, D. J.; Esteva, F. J.; Rivera, E.; Valero, V.; Esparza-Guerra, L.; Priebe, W.; Hortobagyi, G. N. Phase II study of liposomal annamycin in the treatment of doxorubicin-resistant breast cancer. *Cancer Chemother. Pharmacol.* **2002**, *50*, 6−8.

(9) Muggia, F. M.; Blessing, J. A.; Sorosky, J.; Reid, G. C. Phase II trial of the pegylated liposomal doxorubicin in previously treated metastatic endometrial cancer: a gynecologic oncology group study. *J. Clin. Oncol.* **2002**, *20*, 2360−2364.

(10) (a) Kwon, G. S.; Kataoka, K. Block copolymer micelles as long-circulating drug vehicles. *Adv. Drug Delivery Rev*. **1995**, *16*, 295−309. (b) Kwon, G. S. Diblock copolymer nanoparticles for drug delivery. *Crit. Rev. Ther. Drug* **1998**, *15*, 481−512. (c) Jones, M.-C.; Leroux, J.-C. Polymeric micelles − a new generation of colloidal drug carriers. *Eur. J. Pharm. Biopharm*. **1999**, *48*, 101−111. (c) Rapoport, N.; Pitt, W. G.; Sun, H.; Nelson, J. L. Drug delivery in polymeric micelles: from in vitro to in vivo. *J. Controlled Release* **2003**, *91*, 85−95.

(11) Kataoka, K.; Harada, A.; Nagasaki, Y. Block copolymer micelles for drug delivery: design, characterization and biological significance. *Adv. Drug Delivery Rev.* **2001**, *47*, 113−131.

(12) Jones, M.-C.; Leroux, J.-C. Polymer micelles-a new generation of colloid drug carrier. *Eur. J. Phmar. Biopharm.* **1999**, *48*, 101−111.

(13) Yang, L.; Alexandridis, P. Physicochemical aspects of drug delivery and release from polymer-based colloids. *Curr. Opin. Colloid Interface Sci.* **2000**, *5*, 132−143.

(14) Torchilin, V. P.; Weissig, V. Polymeric micelles for the delivery of poorly soluble drugs. *ACS Symp. Ser.* **2000**, *752*, 297−313.

(15) Torchilin, V. P. Structure and design of polymeric surfactant-based drug delivery systems. *J. Controlled Release* **2001**, *73*, 137−172.

(16) Labhasetwar, V.; Song, C.; Levy, R. J. Nanoparticle drug delivery system for restenosis. *Adv. Drug Delivery Rev.* **1997**, *24*, 63−85.

(17) Brigger, I.; Dubernet, C.; Couvreur, P. Nanoparticles in cancer therapy and diagnosis. *Adv. Drug Delivery Rev.* **2002**, *54*, 631−651.

(18) Hans, M. L.; Lowman, A. M. Biodegradable nanoparticles for drug delivery and targeting. *Curr. Opin. Solid State Mater. Sci.* **2002**, *6*, 319−327.

(19) (a) Gref, R.; Minamitake, Y.; Peracchia, M. T.; Trubetskoy, V.; Torchilin, V.; Langer, R. Biodegradable long-circulating polymeric nanospheres. *Science* **1994**, *263*, 1600−1603. (b) Panyam, J.; Labhasetwar, V. Biodegradable nanoparticles for drug and gene delivery to cells and tissue. *Adv. Drug Delivery Rev.* **2003**, *55*, 329−347. (c) Chawla, J. S.; Amiji, M. M. Biodegradable poly(ϵ-caprolactone) nanoparticles for tumor targeted delivery of tamoxifen. *Int. J. Pharm*. **2002**, *249*, 127−138.

(20) Monsky, W. L.; Fukumura, D.; Gohongi, T.; Ancukiewcz, M.; Weich, H. A.; Torchilin, V. P.; Jain, R. K. Augmentation of transvascular transport of macromolecules and nanoparticles in tumors using vascular endothelial growth factor. *Cancer Res.* **1999**, *59*, 4129−4135.

(21) Maeda, H. The enhanced permeability and retention (EPR) effect in tumor vasculature: the key role of tumor-selective macromolecular drug targeting. *Adv. Enzyme Regul.* **2001**, *41*, 189−207.

(22) Jain, R. K. Delivery of molecular medicine to solid tumors: lessons from in vivo imaging of gene expression and function. *J. Controlled Release* **2001**, *74*, 7−25.

(23) Hobbs, S. K.; Monsky, W. L.; Yuan, F.; Roberts, W. G.; Griffith, L.; Torchilin, V. P.; Jain, R. K. Regulation of transport pathways in tumor vessels: role of tumor type and microenvironment. *Proc. Natl. Acad. Sci. U.S.A.* **1998**, *95*, 4607−4612.

(24) Yuan, F.; Dellian, M.; Fukumura, D.; Leuning, M.; Berk, D. D.; Yorchilin, V. P.; Jain, R. K. Vascular permeability in a human tumor xenograft: molecular size dependence and cutoff size. *Cancer Res.* **1995**, *55*, 3752−3756.

(25) Unezaki, S.; Maruyama, K.; Hosoda, J.-I.; Nagae, I.; Koyanagi, Y.; Nakata, M.; Ishida, O.; Iwatsuru, M.; Tsuchiya, S. Direct measurement of the extravasation of poly(ethylene glycol)-coated liposomes into solid tumor tissue by in vivo fluorescence microscopy. *Int. J. Pharm.* **1996**, *144*, 11−17.

(26) Seymour, L. W. Passive tumor targeting of soluble macromolecules and drug conjugates. *Crit. Rev. Ther. Drug Carrier Syst.* **1992**, *9*, 135−187.

(27) Lukyanov, A. N.; Gao, Z.; Mazzola, L.; Torchilin, V. P. Polyethylene glycol-diacyllipid micelles demonstrate increased accumulation in subcutaneous tumors in mice. *Pharm. Res.* **2002**, *19*, 1424−1429.

(28) Moghimi, S. M.; Hunter, A. C.; Murray, J. C. Long-circulating and target-specific nanoparticles: theory to practice. *Pharmacol. Rev.* **2001**, *53*, 283−318.

(29) (a) Bogdanov, A., Jr.; Wright, S. C.; Marecos, E. M.; Bogdanova, A.; Martin, C.; Petherick, P.; Weissleder, R. A long-circulating copolymer in "passive targeting" to solid tumors. *J. Drug Target.* **1997**, *4*, 321−330. (b) Kaul, G.; Amiji, M. Long-circulating poly(ethylene glycol)-modified gelatin nanoparticles for intracellular delivery. *Pharm. Res.* **2002**, *19*, 1061−1067.

(30) Nishiyama, N.; Okazaki, S.; Cabral, H.; Miyamoto, M.; Kato, Y.; Sugiyama, Y.; Nishio, K.; Matsumura, Y.; Kataoka, K. Novel cisplatin-incorporated polymeric micelles can eradicate solid tumors in mice. *Cancer Res.* **2003**, *63*, 8977−8983.

(31) Kwon, G.; Naito, M.; Yokoyama, M.; Okano, T.; Sakurai, Y.; Kataoka, K. Block copolymer micelles for drug delivery: loading and release of doxorubicin. *J. Controlled Release* **1997**, *48*, 195−201.
(32) Chung, J. E.; Yamato, M.; Yokoyama, M.; Aoyagi, T.; Sakurai, Y.; Okano, T. Thermo-responsive drug delivery of polymeric micelles incorporating adriamycin. *Proc. Int. Symp. Controlled Release Bioact. Mater.* **1998**, *25*, 380−381.
(33) Yokoyama, M.; Fukushima, S.; Uehara, R.; Okamoto, K.; Kataoka, K.; Sakurai, Y.; Okano, T. Characterization of physical entrapment and chemical conjugation of adriamycin in polymeric micelles and their design for in vivo delivery to a solid tumor. *J. Controlled Release* **1998**, *50*, 79−92.
(34) Zhang, X.; Burt, H. M.; Von Hoff, D.; Dexter, D.; Mangold, G.; Degen, D.; Oktaba, A. M.; Hunter, W. L. An investigation of the antitumour activity and biodistribution of polymeric micellar paclitaxel. *Cancer Chemother. Pharmacol.* **1997**, *40*, 81−86.
(35) Zhang, X.; Burt, H. M.; Mangold, G.; Dexter, D.; Von Hoff, D.; Mayer, L.; Hunter, W. L. Antitumor efficacy and biodistribution of intravenous polymeric micellar paclitaxel. *Anti-Cancer Drugs* **1997**, *8*, 686−701.
(36) Potineni, A.; Lynn, D. M.; Langer, R.; Amiji, M. M. Poly(ethylene oxide)-modified poly(*β*-amino ester) nanoparticles as a pH-sensitive biodegradable system for paclitaxel delivery. *J. Controlled Release* **2003**, *86*, 223−234.
(37) Bennis, S.; Chapey, C.; Couvreur, P.; Robert, J. Enhanced cytotoxicity of doxorubicin encapsulated in polyhexylcyanoacrylate nanospheres against multi-drug-resistant tumor cells in culture. *Eur. J. Cancer A* **1994**, *30*, 89−93.
(38) Iijima, M.; Nagasaki, Y.; Okada, T.; Kato, M.; Kataoka, K. Core-polymerized reactive micelles from heterotelechelic amphiphilic block copolymers, *Macromolecules* **1999**, *32*, 1140−1146.
(39) Lin, W.; Donglas, R.; Flanagan, R.; Linhardt, R. Accelerated degradation of poly (*ϵ*-caprolactone) by organic amines. *Pharm. Res.* **1994**, *11*, 1030−1035.
(40) Lee, J. H.; Kopeckova, P.; Zhang, J.; Kopecek, J.; Andrade, J. D. Protein resistance of poly(ethylene oxide) surfaces. *Polym. Mater. Sci. and Eng.* **1988**, *59*, 234−238.
(41) Miller, C. R.; Bondurant, B.; McLean, S. D.; McGovern, K. A.; O'Brien, D. F. Liposome-cell interactions in Vitro: Effect of liposome surface charge on the binding and endocytosis of conventional and sterically stabilized liposomes. *Biochemistry* **1998**, *37*, 12875−12883.
(42) Dubois, Ph.; Jerome, R.; Teyssie, Ph. Macromolecular engineering of polylactones and polylactides. 3. Synthesis, characterization, and applications of poly(*ϵ*-caprolactone) macromonomers. *Macromolecules* **1991**, *24*, 977−981.
(43) Shen, Y.; Zhu, S.; Zeng, F.; Pelton, R. Versatile initiators for macromonomer synthesis of acrylates, methacrylates and styrene by atom transfer radical polymerization. *Macromolecules* **2000**, *33*, 5399−5404.
(44) Ge, H.; Hu, Y.; Jiang, X.; Cheng, D.; Yuan, Y.; Bi, H.; Yang, C. Preparation, characterization, and drug release behaviors of drug nimodipine-lodaded poly(*ϵ*-caprolactons)-poly(ethylene oxide)-poly-(*ϵ*-caprolactons) amphiphilic triblock copolymer micelles. *J. Pharm. Sci.* **2002**, *91*, 1463−1473.
(45) Akiyoshi, K.; Deguchi, S.; Moriguchi, N.; Yamaguchi, S.; Sunamoto, J. Self-Aggregates of hydrophobized polysaccharides in water. Formation and characteristics of nanoparticles. *Macromolecules* **1993**, *26*, 3062−3068.
(46) Matyjaszewski, K; Xia, J. Atom transfer radical polymerization. *Chem. Rev.* **2001**, *101*, 2921−2990.
(47) You, L.; Lu, F.; Li, Z.; Zhang, W.; Li, F. Glucose-Sensitive Aggregates Formed by Poly(ethylene oxide)-*block*-poly(2-glucosyl-oxyethyl acrylate) with concanavalin A in dilute aqueous medium. *Macromolecules* **2003**, *36*, 1−4.

BM049874U